Pseudomonas aeruginosa lasI/rhlI quorum sensing genes promote phagocytosis and aquaporin 9 redistribution to the leading and trailing regions in macrophages

Angelika Holm, Thommie Karlsson and Elena Vikström *

Department of Clinical and Experimental Medicine, Faculty of Medicine and Health Sciences, Linköping University, Linköping, Sweden

Pseudomonas aeruginosa controls production of its multiple virulence factors and biofilm development via the quorum sensing (QS) system. QS signals also interact with and affect the behavior of eukaryotic cells. Host water homeostasis and aquaporins (AQP) are essential during pathological conditions since they interfere with the cell cytoskeleton and signaling, and hereby affect cell morphology and functions. We investigated the contribution of *P. aeruginosa* QS genes *lasI/rhlI* to phagocytosis, cell morphology, AQP9 expression, and distribution in human macrophages, using immunoblotting, confocal, and nanoscale imaging. Wild type *P. aeruginosa* with a functional QS system was a more attractive prey for macrophages than the *lasI/rhlI* mutant lacking the production of QS molecules, $3O-C_{12}$-HSL, and C_4-HSL, and associated virulence factors. The *P. aeruginosa* infections resulted in elevated AQP9 expression and relocalization to the leading and trailing regions in macrophages, increased cell area and length; bacteria with a functional QS system *lasI/rhlI* achieved stronger responses. We present evidence for a new role of water fluxes via AQP9 during bacteria–macrophage interaction and for the QS system as an important stimulus in this process. These novel events in the interplay between *P. aeruginosa* and macrophages may influence on the outcome of infection, inflammation, and development of disease.

Keywords: host-bacteria relationship, quorum sensing, *N*-acylhomoserine lactone, innate immunity, macrophage, water homeostasis, aquaporin

Introduction

Tissue resident macrophages can be stimulated by other cells and bacterial products to move to the site of infection, engulf, and kill the bacteria. Cell migration and phagocytosis follow a distinct pattern of repetitive cycles of protrusion of wide, thin lamellipodia, and small finger-like filopodia, resulting in cell polarization with trailing and leading ends in the direction of migration. Thus, to migrate and engulf bacteria, the macrophage must rapidly change its shape and volume; this is driven by an interplay of a highly dynamic plasma membrane, reorganization of actin cytoskeleton and a variety of signaling molecules including phospholipase C, phosphoinositide 3-kinase, Rho family of small GTPases, Ca^{2+} mobilization (Nourshargh and Alon, 2014), fluxes of monovalent ions (Na^+, K^+, Cl^-), and not the least transport of water across the membrane. Although water molecules can diffuse sparsely across the lipid bilayer, membrane water channel proteins, aquaporins (AQP) are key players in this process (Verkman, 2005; Loitto et al., 2009).

Today, 13 mammalian water channels AQP0-AQP12 are known and divided in three different subgroups based on their substrate permeability: orthodox AQP exclusively permeable to water; aquaglyceroporins transporting water, glycerol, and some other small neutral solutes; and subcellular AQP (S-aquaporins, or superaquaporins) (Benga, 2012). A common feature of the AQP is that its water-transporting ability can be blocked by mercury (Hg^{2+}) through its binding to a cysteine thiol localized in the pore (Savage and Stroud, 2007). In human leukocytes, the main aquaglyceroporin AQP9 (Ishibashi et al., 2009) localizes at the leading edge in migrating cells and is required for proper migration (Loitto et al., 2002, 2009). Water fluxes through AQP regulate cell shape and formation of membrane protrusion formation; the mechanism behind this relies on localized influx of water that pushes the membrane outwards allowing the actin cytoskeleton to remodel and elongate and thereby change the cell shape (Karlsson et al., 2013a,b). The involvement of AQP9 has also been implicated in LPS-induced water accumulation in brain and blood-brain barrier perturbation (Wang et al., 2009). In addition, AQP has been identified as one of several universal markers of chronic inflammation in patients with autoimmune diseases (Mesko et al., 2010). Thus, there is a multiple evidence for the importance of water homeostasis and AQPs during infection, inflammation, and bacteria–host cell communication, but the details of the cellular events remain to be further elucidated.

During phagocytosis, macrophages, and neutrophils must rapidly change shape and directional movement, and through their highly flexible membrane and dynamic cytoskeleton be able to form protrusions. Macrophages become activated by many bacterial products, such as formylated peptides and LPS, and more recently bacterial quorum sensing (QS) molecules have been recognized as a novel category of chemoattractants and modulators of phagocytic activity in leukocytes. Thus, it was shown that human neutrophils were stimulated by and migrated toward *N*-acylhomoserine lactone (AHL) molecules (Zimmermann et al., 2006; Karlsson et al., 2012). Moreover, the long-chain fatty acid AHL, 3O-C$_{12}$-HSL stimulate the uptake of

Escherichia coli by neutrophils (Wagner et al., 2007) and yeast particles by macrophages (Vikström et al., 2005).

The QS signaling system primarily enables bacteria to pass on information about population density and collectively regulate the expression of an ensemble of genes (Williams and Cámara, 2009; Rutherford and Bassler, 2012). The Gram-negative pathogen *P. aeruginosa* harbors at least three subordinated QS systems: two of LuxI/LuxR-type which are *N*-acylhomoserine lactone (AHL) dependent and one quinolone-type system (PQS). In the first, the LuxI homolog LasI synthesizes the diffusible *N*-3-oxo-dodecanoyl-*L*-homoserine lactone (3O-C$_{12}$-HSL) that is recognized by the LuxR homolog, cytoplasmic receptor LasR (Moré et al., 1996; Parsek et al., 1999). In the second, the LuxI homolog RhlI produces another AHL, *N*-butyryl-*L*-homoserine lactone (C$_4$-HSL) that is detected by the cytoplasmic receptor RhlR (Ochsner et al., 1994; Pearson et al., 1995). LasR and RhlR regulate transcription and maintain the activity of about 300 genes in the large *P. aeruginosa* genome. These multiple genes encode the production of rhamnolipids, surface-active molecules important for the late stage of biofilm formation (Ochsner et al., 1994; de Kievit, 2009), and extracellular virulence factors (elastases, proteases, lectins, pyocyanin, and exotoxin A) that can destroy host tissues and initiate infection and inflammation (Gambello and Iglewski, 1991; Toder et al., 1991; Gambello et al., 1993; Schuster et al., 2003). Bacterial QS can also elicit inter-kingdom signaling by affecting the behavior of eukaryotic cells, which has been addressed by many researchers (Jarosz et al., 2011; Teplitski et al., 2011; Holm and Vikström, 2014).

The aim of this study was to investigate the contribution of *P. aeruginosa* QS genes *lasI/rhlI* to phagocytosis, cell morphology, AQP9 expression, and distribution in macrophages, using immunoblotting, confocal, and nanoscale imaging.

Materials and Methods

Ethics Statement

The study was carried out according to the Declaration of Helsinki. Human blood and buffy coat was collected by employees at the Blood Bank, Linköping University Hospital, Sweden. A written agreement for research use of blood was obtained from all donors. The study did not require ethical approval according to paragraph 4 of the Swedish law (2003:460; http://www.lagboken.se/dokument/Lagar-och-forordningar/406 0/Lag-2003_460-om-etikprovning-av-forskning-som-avser-man niskor?id=64991) on Ethical Conduct in Human Research, since blood donation is assumed as negligible risk to the donors and only anonymized blood samples were delivered to the researchers.

Human Primary Monocyte-derived Macrophages

Monocytes were obtained from buffy coat from healthy blood donors (Blood Bank, Linköping University Hospital). The buffy coat was mixed 50/50 with cold 0.9% NaCl and a leukocyte concentrate was obtained using a Lymphoprep gradient (Axis Shield, Oslo, Norway) by centrifugation for 40 min at 480 × g at room temperature (RT). The mononuclear cell layer was collected, washed thrice in cold PBS, pH7.3 with 0.1 IE/ml

heparin (LEO Pharma, Ballerup, Denmark) and thrice in cold calcium-free Krebs-Ringer Glucose buffer, KRG (120 mM NaCl, 4.9 mM KCl, 1.2 mM MgSO$_4$, 8.3 mM KH$_2$PO$_4$, 10 mM glucose) to remove the density gradient. Cells were seeded in Dulbecco's modified Eagle's medium, DMEM, with 25 mM HEPES, 100 U/ml penicillin and 100 µg/ml streptomycin (Life Technologies, Grand Island, NY) and left to adhere for 1.5–2 h at 37°C in 5% CO$_2$. Unbound cells were washed out with calcium-containing KRG, KRG+Ca^{2+} (as above with addition of 1 mM CaCl$_2$) at 37°C. The adherent monocytes were allowed to differentiate in DMEM with 10% human serum (pooled from five healthy donors, Blood Bank, Linköping University Hospital) and 80 µM L-glutamine (Life Technologies). After 7–8 days, the cells were considered to be differentiated macrophages, based on their morphology and phagocytic activity. For experiments, macrophages were detached with trypsin-EDTA (Life Technologies), washed, counted, and reseeded at concentration 10^6 cells/well in six-well plates for further immunoblotting or at 5×10^4 on glass coverslips (thickness 0.17 ± 0.01, 13 mm-diameter; Karl Hecht Assistent, Sondheim, Germany) for phagocytosis and imaging. Cells were left to adhere in DMEM as above for 2 h at 37°C in 5% CO$_2$, and then starved overnight in DMEM with 25 mM HEPES without serum and antibiotics.

Bacterial Strains

Two *P. aeruginosa* strains used were wild-type PAO1 and its double mutant PAO1 *lasI-/rhlI-* which is also called PAO1-JP2, PAO $\Delta rhlI$::Tn501 *lasI*::Tc^r, Hg^r (Brint and Ohman, 1995; Pearson et al., 1997) and defective in the synthesis of QS molecules 3O-C$_{12}$-HSL and C$_4$-HSL. Both strains were constitutively expressing the stable green fluorescent protein, GFP, and were a kind gift from Prof. Thomas Bjarnsholt (University of Copenhagen, Denmark). Bacteria were grown in Luria-Bertani (LB) liquid medium or on agar plates containing 150–200 µg/ml carbenicillin to maintain a stable expression of GFP; tetracycline (50 or 300 µg/ml) and mercuric chloride (7.5 or 15 µg/ml) were added (all from Sigma Aldrich, St. Louis, MO) to maintain the *lasI-/rhlI-* mutations.

AHL Synthesis

Two AHL, long-chain fatty acid 3O-C$_{12}$-HSL (MW297), and short-chain C$_4$-HSL (MW171) were synthesized by Prof. Peter Konradsson and co-workers (Linköping University, Sweden) as previously described (Chhabra et al., 2003). Both AHL are structurally and functionally identical to those obtained from *P. aeruginosa* cultures; they were checked for identity and purity by HPLC, and their biological activity as QS molecules was validated by the bioassay described earlier (Surette and Bassler, 1998). Stock AHL were dissolved in dimethylsulfoxide (DMSO).

Bacterial Infection and Treatment with AHL and AQP Blockers

Before infection, bacteria were grown in LB medium overnight at 37°C with shaking, re-suspended in 0.9% NaCl to an optical density of 0.09 at 600 nm, OD$_{600}$ (1 × 10^8 CFU/ml) and further diluted in DMEM with 25 mM HEPES without serum and antibiotics. Macrophages, at a concentration 10^6 cells/well or
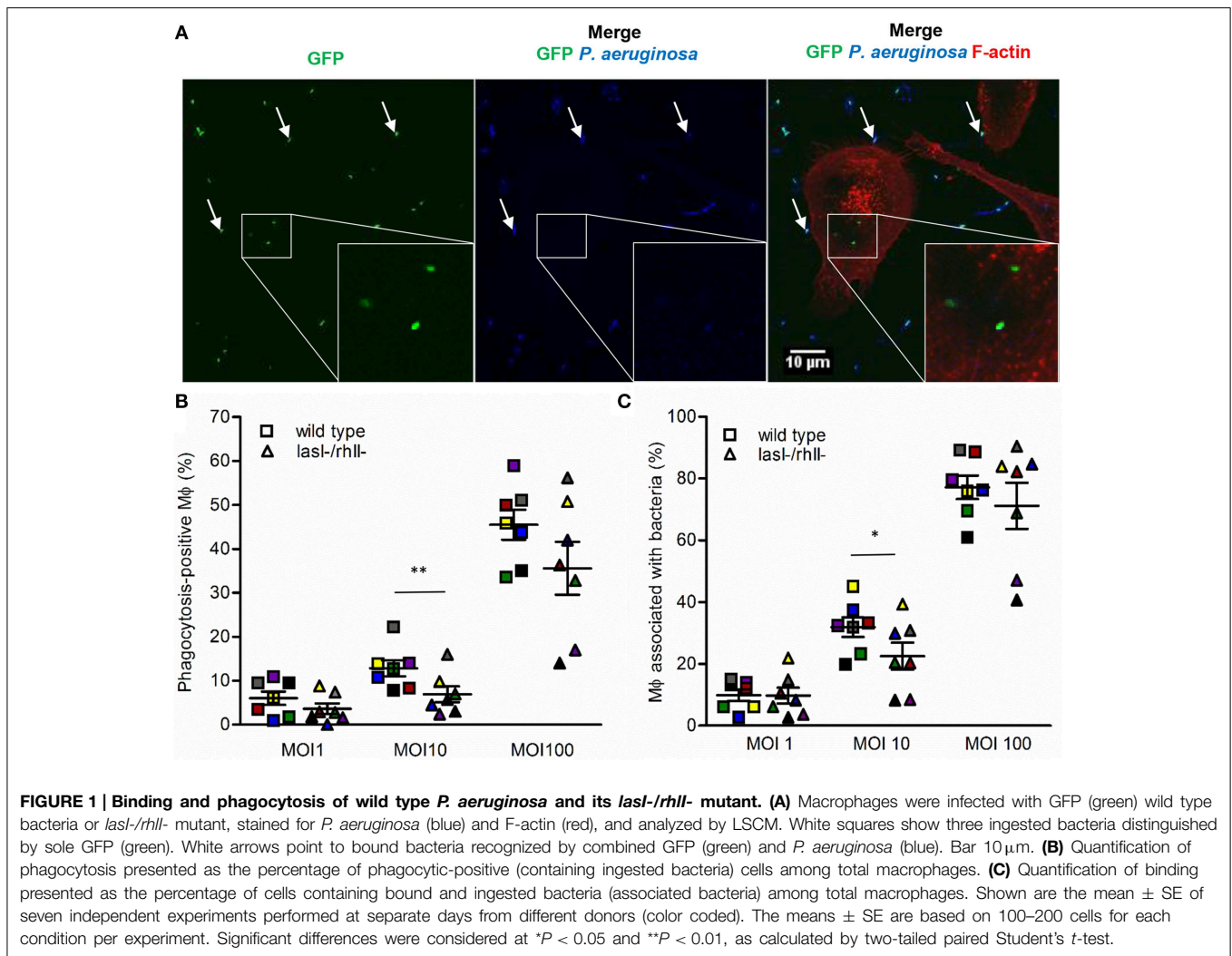
5 × 10^4 on glass coverslips, were infected with bacteria at multiplicities of infection (MOI) 1, 10, and 100 in fresh DMEM, incubated for 1 h at 37°C in 5% CO$_2$ and further proceeded for the phagocytosis assay, imaging or immunoblotting. To examine the functional complementation of phagocytosis, macrophages were pretreated with a mixture of 25 µM C$_4$-HSL and 50 µM 3O-C$_{12}$-HSL (in 0.02% DMSO) for 4 h before infection at MOI 10. To assess the role of AQP, two kinds of water influx inhibitors were used: HgCl$_2$, which blocks water transport activity of most AQP through thiol binding to a pore-localized cysteine (Savage and Stroud, 2007); and HTS13286 a specific peptide inhibitor of AQP9 (Jelen et al., 2011; Karlsson et al., 2013a; Wacker et al., 2013). Macrophages were pretreated with 1 or 5 µM HgCl$_2$ (Sigma Aldrich) or 25 µM HTS13286 (Maybridge, Cornwall, UK) for 20 min. As vehicle for HTS13286, 0.25% DMSO was used.

Phagocytosis Assay

Samples on glass cover slips were washed with KRG+Ca^{2+}, fixed with 4% paraformaldehyde (Sigma Aldrich) for 20 min at RT and blocked in 1% BSA. To label non-ingested and surface-attached bacteria, the samples were incubated for 1 h at RT with rabbit anti-*Pseudomonas* antibodies (#PAI-73116, Thermo Scientific, Rockford, IL), diluted 1:800, washed and incubated with Alexa Fluor 635-conjugated goat anti-rabbit antibodies (Life Technologies), 1:1000 for 1 h at RT. The cells were permeabilized in 0.1% Triton X-100 in PBS (Sigma Aldrich) for 5 min at RT, washed again and stained for 20 min at RT with Alexa Fluor 568-conjugated phalloidin for cytoskeleton F-actin labeling (Life Technologies), diluted 1:40 in PBS from 200 units/ml methanol stock solution. After washing, the speciments were mounted in ProLong Gold antifade reagent (Life Technologies) and examined through a 63 × oil immersion objectives with NA 1.40 in a fluorescence microscope Zeiss Axio Observer Z1 with confocal system Zeiss LSM700 and Zeiss ZEN software (Carl Zeiss, Jena, Germany). Random images were chosen through the red channel (F-actin) to avoid biases for only selecting phagocytic cells with bacteria. Completely ingested bacteria were distinguished by their sole GFP fluorescence (green); bound and non-ingested ones were recognized by combined GFP (green) and Alexa Fluor 647 (blue) color (**Figure 1A**). Macrophages containing ingested bacteria were counted as phagocytosis-positive cells (**Figure 1A,** shown in white squares and inserts); and macrophages with adherent (**Figure 1A,** pointed by white arrows) and/or ingested bacteria were counted as macrophages associated with bacteria. To quantitate, Fidji software (NIH, Bethesda, MD) was used; binding- and phagocytic activities were presented as the percentage of phagocytosis-positive macrophages among total cells. The results from four-seven independent experiments, performed on separate days and from different blood donors were expressed as the mean ± SE; about 100–200 macrophages per sample were counted. The images and measurements were taken by two independent observers or by blinding of the samples.

LSCM, SIM, and STED Imaging

The specimens for imaging were fixed and stained to label non-ingested or surface-attached bacteria, as described above

FIGURE 1 | Binding and phagocytosis of wild type *P. aeruginosa* and its *lasI-/rhlI-* mutant. (A) Macrophages were infected with GFP (green) wild type bacteria or *lasI-/rhlI-* mutant, stained for *P. aeruginosa* (blue) and F-actin (red), and analyzed by LSCM. White squares show three ingested bacteria distinguished by sole GFP (green). White arrows point to bound bacteria recognized by combined GFP (green) and *P. aeruginosa* (blue). Bar 10 μm. **(B)** Quantification of phagocytosis presented as the percentage of phagocytic-positive (containing ingested bacteria) cells among total macrophages. **(C)** Quantification of binding presented as the percentage of cells containing bound and ingested bacteria (associated bacteria) among total macrophages. Shown are the mean ± SE of seven independent experiments performed at separate days from different donors (color coded). The means ± SE are based on 100–200 cells for each condition per experiment. Significant differences were considered at *$P < 0.05$ and **$P < 0.01$, as calculated by two-tailed paired Student's *t*-test.

for the phagocytosis assay. Then, the samples were stained with rabbit anti-AQP9 antibodies (#ab84828-100, Abcam, UK) and Atto647N (fluorophore for STED) secondary antibodies (Active Motif, Carlsbad, CA), and mounted in ProLong Gold antifade reagent (Life Technologies). For laser scanning confocal microscopy (LSCM), the specimens were examined through a 63 × oil immersion objectives with NA 1.40 in a fluorescence microscope Zeiss Axio Observer Z1 with confocal system Zeiss LSM 700 and Zeiss ZEN software (Carl Zeiss, Jena, Germany). For structured illumination microscopy (SIM), yielding resolution of around 100 nm which is double, than could be achieved in LSCM, the samples were examined in a fluorescence microscope Zeiss LSM 780 with ELYRA S.1 system (Carl Zeiss, Jena). For nanoscale visualization, allowing capture very fine structural details with a resolution of around 20–40 nm, which is 5–10 times higher than can be achieved in LSCM, the specimens were examined in a Leica TCS STED Stimulated Emission Depletion confocal microscope with a pulsed IR-laser and a 100 × oil immersion objective (Leica Microsystems, Mannheim, Germany). These advanced techniques are based on either probing the samples with spatially modulated illumination

or switching fluorophores on and off sequentially in time (Blom and Brismar, 2014). Fluorescence intensity, cell area, and length were measured and quantified using the Fidji software (NIH). The images and measurements were taken by two independent observers or by blinding of the samples.

Preparation of Total Cell Lysates, SDS-PAGE, and Immunoblotting

Samples were rinsed with PBS, pH 7.6 and lysed with cold RIPA buffer (1% NP-40, 1% deoxycholic acid sodium salt, 0.1% SDS, 150 mM NaCl, 10 mM Tris pH 7.4, 10 mM EDTA pH 8.0 dissolved in PBS) containing 25 U nuclease (Thermo Scientific), 1 mM phenyl-methyl-sulfonyl-fluoride, 1 mM Na_3VaO_4, 25 mM NaF (Sigma), protein inhibitors Complete (Roche Diagnostics, Mannheim, Germany). Cell lysates were homogenized through a 21-gauge needle, centrifuged at 18,000 g for 30 min at 4°C, and the supernatants collected. The protein concentrations in lysates were measured with the Bio-Rad D_C protein assay (Bio-Rad Laboratories, Hercules, CA). The samples were diluted in Laemmli sample buffer at equal protein concentrations, heated for 5 min at 95°C and loaded on 4–12% SDS-polyacrylamide

gels (Lonza, Rockland, ME). After separation, proteins were electrophoretically transferred to a PVDF membrane (Millipore, Bedford, MA); the quality of the transfer was monitored by Ponceau S staining (Sigma Aldrich). The membranes were blocked in 5% non-fat milk in PBS pH 7.6, with 0.18% Tween-20 for 1 h at RT and incubated overnight at 4°C with rabbit anti-AQP9 antibodies (#ab85910 Abcam), diluted 1:2000 or mouse anti-GAPDH antibodies (Millipore, Temecula, CA) in blocking buffer. After washing, they were incubated for 1 h at RT with IRDye 800CW goat anti-rabbit or IRDye 680CW goat anti-mouse antibodies (LI-COR Biosciences, Cambridge, UK), diluted 1:10,000 and washed extensively. The signals were detected and quantified by Odyssey CLx and the Image Studio software (LI-COR).

mRNA Array Analysis

Cells were rinsed with PBS, pH 7.6 and lysed with TRIzol (Life Technologies) to obtain total RNA. The Affymetrix human arrays and mRNA expression profiling were performed by Atlas Biolabs GmbH (Berlin, Germany).

Statistical Analysis

Data are presented as mean $\pm$ SE. Data from the phagocytosis assays were analyzed using paired, two-tailed t-test. Whole cell and over the cell AQP9 fluorescence intensity were analyzed using unpaired, two-tailed t-test when comparing control vs. infected samples and one-tailed t-test for comparison of wild type and $lasI$-/$rhlI$- mutant. The numbers (n) are specified in the figure legends. $P < 0.05$ were considered significant.

Results

More Effective Binding and Phagocytosis of Wild Type *P. aeruginosa* than of Its *lasI-/rhlI-* Mutant

QS signal molecules with a long fatty-acid chain and an intact ring, e.g., 3O-C_{12}-HSL and 3O-C_{10}-HSL, can by themselves affect leukocytes chemotaxis (Zimmermann et al., 2006; Karlsson et al., 2012) and phagocytosis of yeast and *E.coli* (Vikström et al., 2005; Wagner et al., 2007). In the present phagocytosis model using *P. aeruginosa* bacteria as preys, we studied comparatively how wild-type and *lasI-/rhlI-* mutant, defective in the synthesis of 3O-C_{12}-HSL and C_4-HSL are phagocytized by human macrophages (**Figure 1A**). After 1-h infection, we observed an increased binding and phagocytic activity in macrophages treated with wild-type bacteria compared to with *lasI-/rhlI-* mutant at all MOI (**Figures 1B,C**). Quantitatively, wild-type bacteria at MOI 10 induced a significant, 1.42- and 1.86-fold greater binding and phagocytic capacity, respectively, in contrast to the QS defective mutant. At MOI 1 and 100, the patterns of macrophage activity to adhere and engulf wild-type *P. aeruginosa* were also increased, but not significantly compared to mutant (**Figures 1B,C**). This can be explained by a MOI-dependent effect on the capacity and effectiveness of migration, binding, and phagocytosis, which rely on an optimal concentration of the prey, the chemical nature, and gradient of chemotactic ligands released by bacteria, resulting in either attraction or repulsion of macrophages. The number

of adherent and ingested bacteria per individual phagocytizing macrophage were very similar (**Figures S1A,B**).

We next determined whether phagocytosis activity could be functionally complemented by pre-treatment of macrophages with synthetic C_4-HSL and 3O-C_{12}-HSL before infection with either wild type or *lasI-/rhlI-* mutant. As shown in **Figure 2**, in one of four independent experiments, marked with orange, stimulation with AHL was able to elevate phagocytosis and rescue the difference seen in the phagocytic activity between the wild type and the mutant. This partial inconsistence can be explained by donor-specific variations in the macrophages that can display different capacities and functions, including migration and phagocytosis. Taken together, this suggests that wild type *P. aeruginosa* is more attractive prey for macrophages or stimulate their own ingestion compared to the strain with a mutation in the *lasI* and *rhlI* genes and lacking synthesis of 3O-C_{12}-HSL and C_4-HSL and hence many virulence factors.

AQP9 Protein Levels Are Increased in Macrophages Infected with *P. aeruginosa*

For migration into tissues, human leukocytes must to be able to quickly change their morphology and volume, which is largely driven by water fluxes across the membrane through aquaporins, primarily AQP9 in human leukocytes (Loitto et al., 2002, 2009; Karlsson et al., 2013a). Since macrophage phagocytosis of bacteria with intact QS system was increased, we addressed whether AQP9 was involved in this process by investigating the effects of the wild type *P. aeruginosa* and *lasI-/rhlI-* mutant on the protein expression levels of AQP9 in macrophages. This was analyzed by immunoblotting for AQP9 and GAPDH, as a loading control (**Figure 3A**), with subsequent quantification of
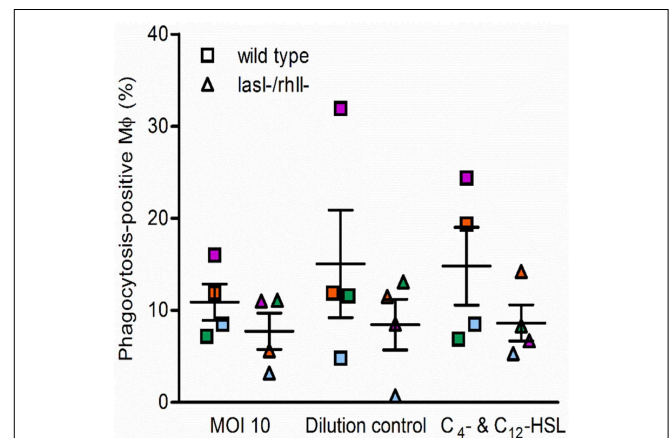

FIGURE 2 | Functional complementation of phagocytosis with AHL. Macrophages were pretreated with 25 μM C_4-HSL and 50 μM 3O-C_{12}-HSL (C_4- C_{12}-HSL), or 0.02% DMSO as a vehicle control (Dilution control), or not-pretreated (MOI 10) for 4 h before 1-h infection with *P. aeruginosa* wild type or *lasI-/rhlI-* mutant, at MOI 10. Quantification of phagocytosis presented as the percentage of phagocytic-positive (containing ingested bacteria) cells among total macrophages. Shown are mean ± SE of four independent experiments performed at separate days from four different donors (color coded). The means ± SE are based on 100–200 cells for each condition per experiment.

the density of the specific bands (**Figure 3B**). Here, treatment with wild type *P. aeruginosa* and *lasI-/rhlI-* mutant at all MOI caused a significantly increased expression of AQP9 compared to non-infected control macrophages. Wild type bacteria seems to cause a more pronounced increase in the expression level of AQP9 than its QS defective mutant, but no significant differences were found. To assess the relationship between protein and mRNA expression levels, we assessed mRNA for all AQP types, AQP0-12. After infection with wild type *P. aeruginosa* and *lasI-/rhlI-* mutant for 1 h, mRNA levels were slightly affected for AQP0, 1, 2, 3, 8, 11, and 12, with exception for AQP4, 5, 6, 7, 9, and 10 that maintained near to the basal expression level (**Table S1**).

Effects of *P. aeruginosa* on the Cellular Distribution of AQP9

During locomotion, the cellular distribution and dynamics of AQP9 has been shown to be crucial in promoting protrusion activity by accumulation in membrane domains and preceding formation of filopodia, blebs, and lamellipodia (Loitto et al.,

FIGURE 3 | **AQP9 protein levels are increased in macrophages infected with *P. aeruginosa*. (A)** Macrophages were either non-infected (C) or infected with wild type *P. aeruginosa* or *lasI-/rhlI-* mutant at MOI 1, 10, and 100 for 1 h. Total cellular protein extracts were analyzed with Western blot for AQP9, 31 kDa (lower, green bands) and GAPDH, 36 kDa as a loading control (upper, red bands). The blots are from one representative of four independent experiments. **(B)** Densitometric analysis. Values are mean ± SE percentage of AQP9 density relative to the loading GAPDH control from four independent experiment performed at separate days from four different donors. Significant differences are indicated when *$P < 0.05$ and **$P < 0.01$, as analyzed by Student's *t*-test.

2002; Karlsson et al., 2011, 2013a,b). Therefore, we investigated whether *P. aeruginosa* affected the cellular distribution and localization of AQP9 using confocal imaging (**Figure 4A**). The control, non-infected macrophages displayed low levels of AQP9 in the cytoplasmic region. But after 1-h infection with wild type *P. aeruginosa* and *lasI-/rhlI-* mutant at all MOI, we observed remarkable alterations in intensity and localization of AQP9. Here, the whole cell AQP9 fluorescence intensity was significantly higher in all infected macrophages compared to untreated control (**Figure 4B**). Interestingly, wild type *P. aeruginosa* at MOI 10 lead to significantly increased whole cell AQP9 fluorescence intensity than the *lasI-/rhlI-* mutant. In general, bacteria-infected macrophages became more polarized in their morphology, and measurements of AQP9 fluorescence intensity over the macrophages in the direction of polarization (as indicated by white arrow in **Figure 4A**), demonstrated significant re-localization of AQP9 in infected cells compared to uninfected controls. The infected cells displayed a more AQP9 in the front and the back of the cell, whereas the control have a smoother, more evenly distributed profile of AQP9 (**Figures 4C,D**). Taken together, *P. aeruginosa* infection lead to increased cellular distribution and re-localization of AQP9 to the leading and trailing regions in human macrophages, and bacteria with functional QS system may contribute more to this process.

P. aeruginosa Affects Cell Morphology in Macrophages

Since *P. aeruginosa* infection caused increased cellular distribution and re-localization of AQP9 in macrophages, parallel changes in their morphology and volume driven by water fluxes across the AQP may occur. The cell area was significantly larger at all MOIs after infection with wild type bacteria compared to uninfected control (**Figure 5A**). *P. aeruginosa lasI-/rhlI-* mutant had smaller effect on the cell area and no significant differences compared to uninfected control (**Figure 5A**). The approximated cell length, measured in the direction of polarization, shown in **Figure 4A**, was significantly greater in macrophages infected with wild type *P. aeruginosa* and *lasI-/rhlI-* mutant at MOI 1 and 10 compared to untreated control macrophages (**Figure 5B**). These data confirm that the *P. aeruginosa*-induced increase in cellular distribution and re-localization of AQP9 in macrophages are paralleled with changes in cell size.

Nanoscale Visualization of AQP9 in Macrophages during *P. aeruginosa* Infections

To further study the details of *P. aeruginosa*-induced alterations in AQP9 distribution and localization in human macrophages, we used two novel super-resolution imaging techniques, giving much sharper images. These were structured illumination microscopy (SIM), yielding resolution of around 100 nm (**Figure S2**), and stimulated emission depletion (STED), allowing a further increased resolution of around 20–40 nm (**Figure 6A**). After 1-h infection with wild type *P. aeruginosa* at MOI 10, we observed more distinct AQP9 localization in the
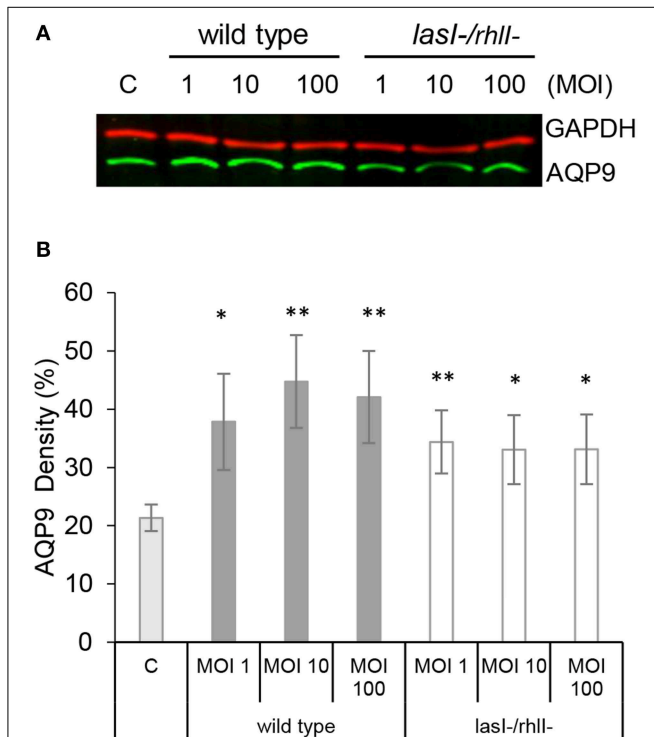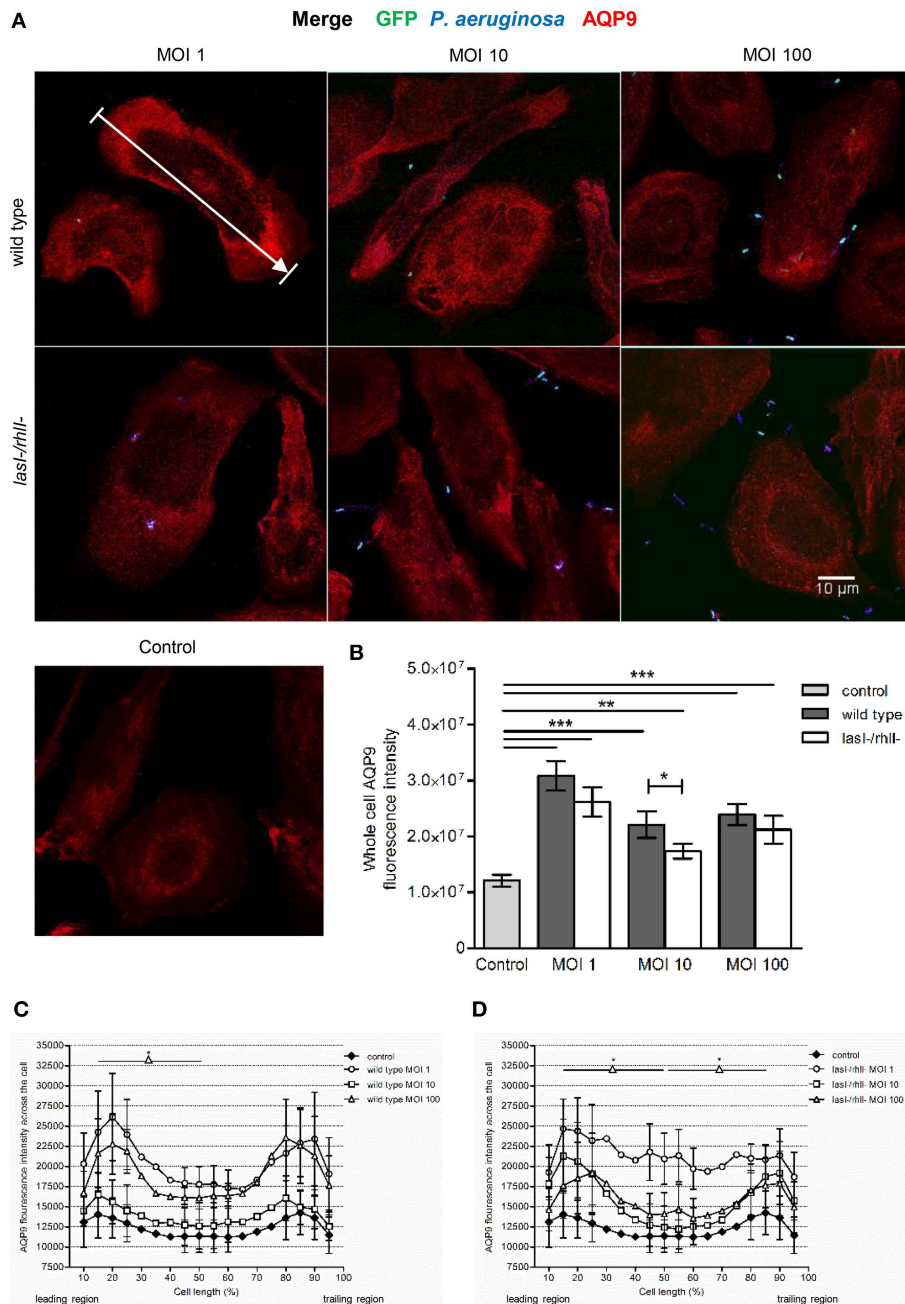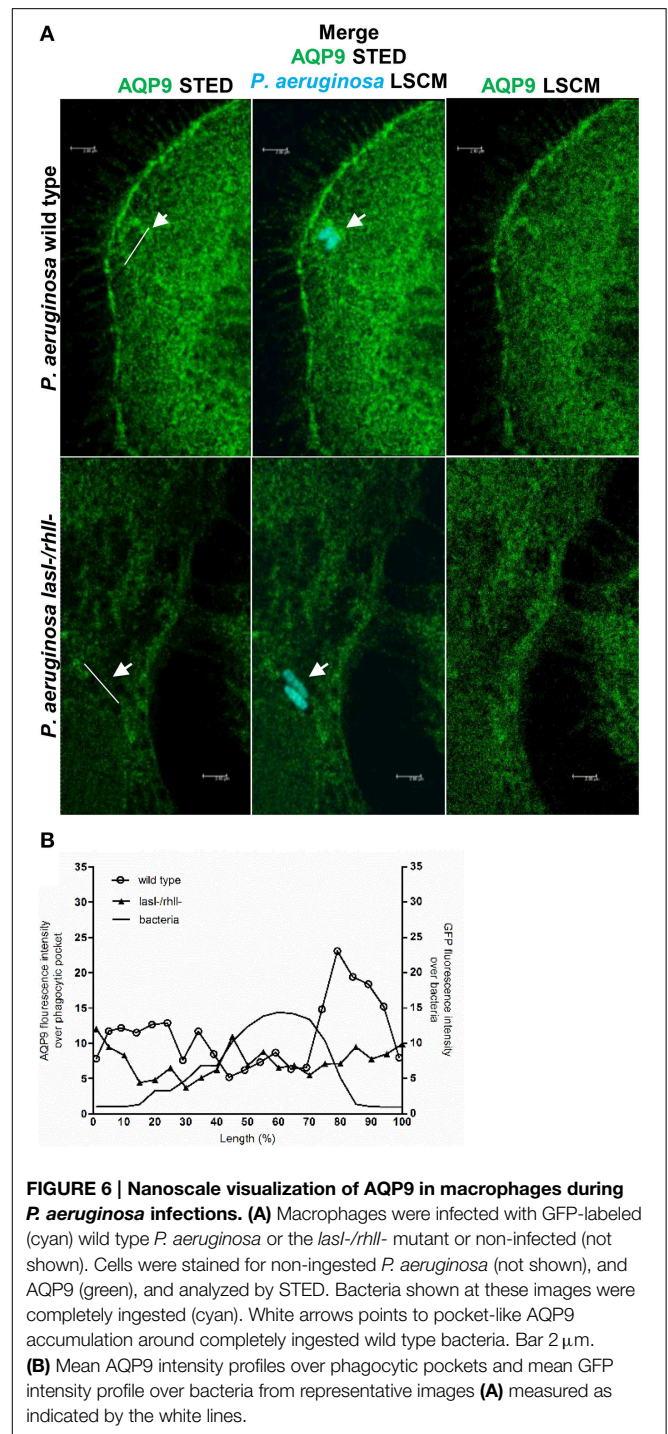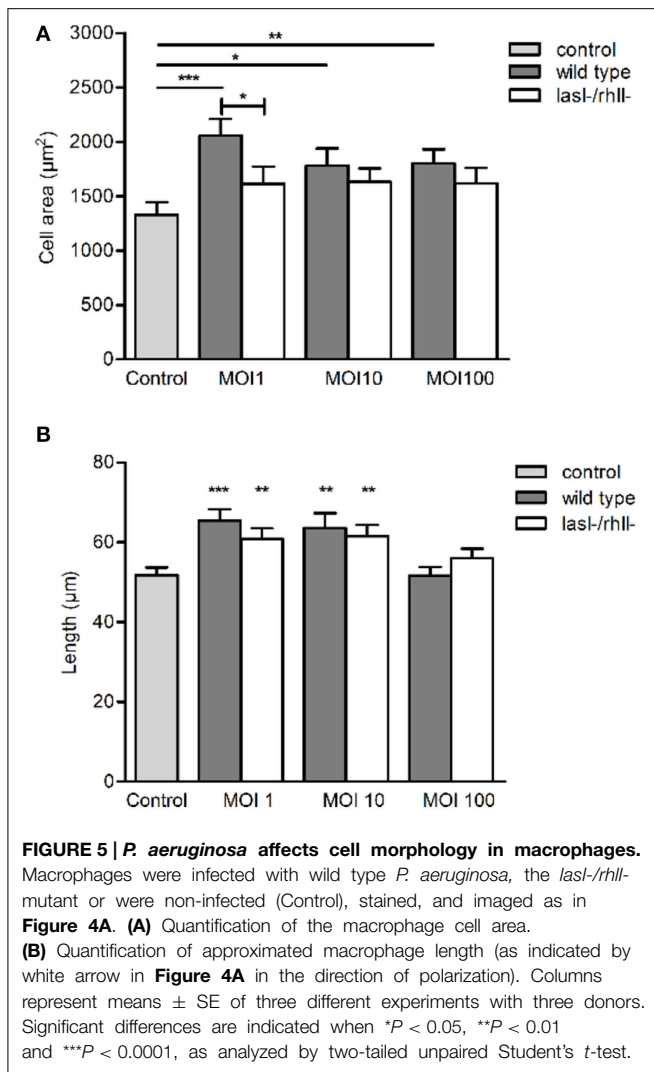
FIGURE 4 | Effects of *P. aeruginosa* on the cellular distribution of AQP9. (A) Macrophages were infected with GFP (green) wild type *P. aeruginosa,* the *lasI-/rhlI-*mutant, or non-infected (Control), stained for *P. aeruginosa* (blue), AQP9 (red) and analyzed by LSCM. The data are from one of at least three independent experiments. Bar 10 μm. **(B)** Quantification of AQP9 immunofluorescence intensity measured as a total integrated intensity of whole macrophage area, of at least 30 cells for each condition. Data are from at least three experiments performed at separate days from different donors. Columns represent means ± SE. Significant differences are indicated when **$P < 0.01$ and ***$P < 0.0001$, as analyzed by two-tailed unpaired Student's *t*-test. **(C,D)** Quantification of AQP9 immunofluorescence intensity profile measured across the cells in the direction of polarization as indicated by white arrow in **(A)**. Significant differences are indicated when *$P < 0.05$, as analyzed by one-tailed unpaired Student's *t*-test.

cytoplasm at peripheral regions in vicinity of leading- and trailing- edges and in protruding structures, *i.e.,* in filopodia and lamellae. In addition, the wild type strain triggered a pocket-like AQP9 accumulation around intracellular bacteria. By contrast, the *lasI-/rhlI-* mutant induced smaller and modest

effects on the AQP9 nanostructure (white arrow **Figures 6A,B**). Thus, super-resolution imaging revealed distinct details in nanoscale structural organization of AQP9 in macrophages during phagocytosis of wild type *P. aeruginosa* and the *lasI-/rhlI-*mutant.

FIGURE 5 | *P. aeruginosa* affects cell morphology in macrophages.
Macrophages were infected with wild type *P. aeruginosa,* the *lasI-/rhlI-*
mutant or were non-infected (Control), stained, and imaged as in
Figure 4A. (A) Quantification of the macrophage cell area.
(B) Quantification of approximated macrophage length (as indicated by
white arrow in **Figure 4A** in the direction of polarization). Columns
represent means ± SE of three different experiments with three donors.
Significant differences are indicated when *$P < 0.05$, **$P < 0.01$
and ***$P < 0.0001$, as analyzed by two-tailed unpaired Student's *t*-test.

FIGURE 6 | Nanoscale visualization of AQP9 in macrophages during
P. aeruginosa infections. (A) Macrophages were infected with GFP-labeled
(cyan) wild type *P. aeruginosa* or the *lasI-/rhlI-* mutant or non-infected (not
shown). Cells were stained for non-ingested *P. aeruginosa* (not shown), and
AQP9 (green), and analyzed by STED. Bacteria shown at these images were
completely ingested (cyan). White arrows points to pocket-like AQP9
accumulation around completely ingested wild type bacteria. Bar 2 µm.
(B) Mean AQP9 intensity profiles over phagocytic pockets and mean GFP
intensity profile over bacteria from representative images (A) measured as
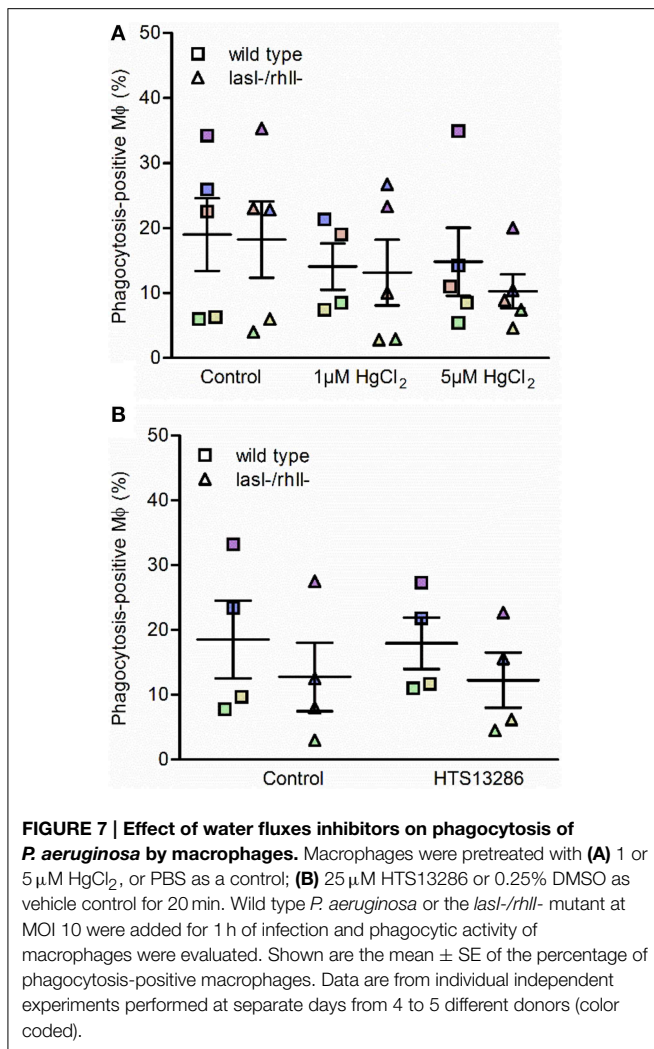indicated by the white lines.

Effect of Water Fluxes Inhibitors on Phagocytosis of *P. aeruginosa* by Macrophages

Next, we investigated whether inhibition of water transport
via AQP and particularly AQP9 influenced the phagocytosis of
P. aeruginosa by macrophages. To do so, macrophages were
pretreated for 20 min with 1 or 5 µM $HgCl_2$ to block most AQP
and 25 µM HTS13286 to inhibit AQP9, and PBS or 0.25% DMSO
as vehicle control. We observed that the inhibition of water
fluxes via most AQP only slightly prevented the phagocytosis
of bacteria (**Figure 7A**), while AQP9 blocker failed to get a
clear effect (**Figure 7B**). Looking at the responses of the cells
from individual donors, those marked with violet, blue, and
brown, there was an inhibitory effect at 5 µM $HgCl_2$. For
the specific AQP9 inhibitor, this was seen only for the "high
responder" violet cells. These data suggest that water transport
across the membrane through AQP only partly facilitated the
phagocytosis of *P. aeruginosa* by macrophages, suggesting that
other crucial cellular signaling pathways were engaged in the
event.

Discussion

The outcome of infections and development of disease depend
on both host defense and bacterial traits, and where QS
plays a critical role in pathogenesis of bacteria to favor their
persistence. Here, we demonstrate that wild type *P. aeruginosa*
is a more attractive target for macrophages to adhere to and
phagocytize than *lasI-/rhlI-* mutant defective in production of

FIGURE 7 | Effect of water fluxes inhibitors on phagocytosis of
***P. aeruginosa* by macrophages.** Macrophages were pretreated with **(A)** 1 or
5 μM $HgCl_2$, or PBS as a control; **(B)** 25 μM HTS13286 or 0.25% DMSO as
vehicle control for 20 min. Wild type *P. aeruginosa* or the *lasI-/rhlI-* mutant at
MOI 10 were added for 1 h of infection and phagocytic activity of
macrophages were evaluated. Shown are the mean ± SE of the percentage of
phagocytosis-positive macrophages. Data are from individual independent
experiments performed at separate days from 4 to 5 different donors (color
coded).

QS signal molecules 3O-C_{12}-HSL and C_4-HSL, and thereby
multiply virulence factors (**Figure 1**). Furthermore, *P. aeruginosa*
induced increased expression, distribution and re-organization of
AQP9 (**Figures 4, 6**) paralleled with changes in macrophage size
and morphology (**Figure 5**), that together can facilitate motility,
migration and phagocytosis. Thus, we propose novel roles for the
QS system and AQP in the interaction between *P. aeruginosa*
and human macrophages, which may have an influence on the
outcome of infection, inflammation, and development of disease
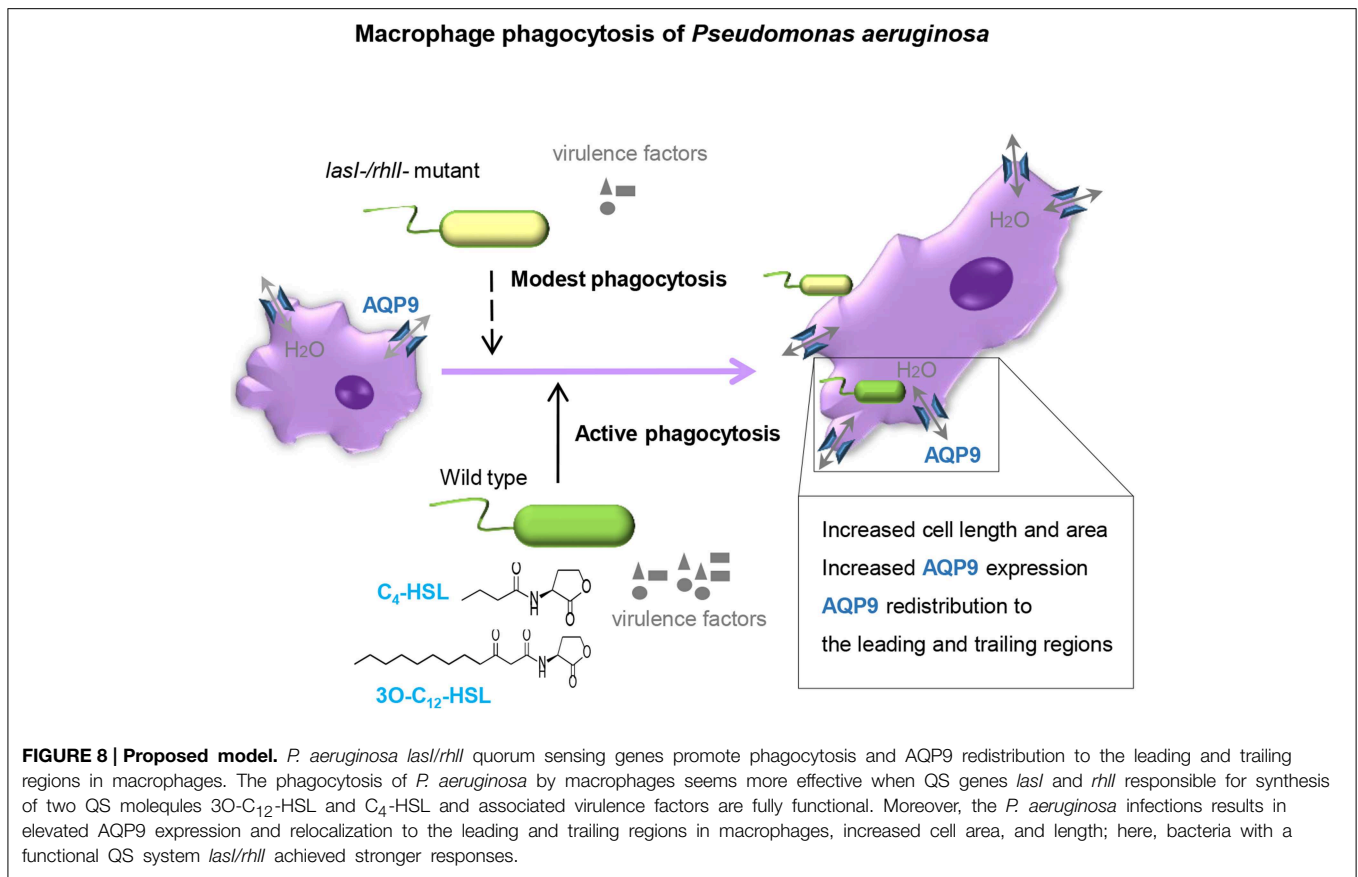(**Figure 8**).

P. aeruginosa is a highly adaptable Gram-negative bacterium,
involved in both acute and chronic infections, typically in
patients having compromised epithelial barriers and immune
systems or the genetic disorder cystic fibrosis. *P. aeruginosa*
is a common cause of lung, skin, ocular, urinary tract,
and gastrointestinal tract infections. Experimental models of
P. aeruginosa in acute pulmonary and burn-wound infections
in mice have shown, that strains containing mutations in one
or more of the QS genes are less virulent than wild-type
bacteria (Tang et al., 1996; Rumbaugh et al., 1999; Pearson
et al., 2000). QS signals have been detected in the sputum from

cystic fibrosis patients (Singh et al., 2000) typically colonized
with *P. aeruginosa*, *Burkholderia* species and *Staphylococcus
aureus*. Clinical *P. aeruginosa* cystic fibrosis isolates often
harbor mutations in QS system which gives them advantages to
survive in low amino acid pulmonary environment, increased β-
lactamase activity and hereby better adaptation during chronic
respiratory infections. In contrast, *Burkholderia* QS mutants were
far less frequent during chronic infections, which can have a
competitive advantage for these species *in vivo* (Cullen and
McClean, 2015).

Macrophages may sense and recognize *P. aeruginosa*
harboring a functional QS system as a danger signal and thereby
perhaps mount more effective phagocytosis to eliminate bacteria
(**Figure 1**). Stimulation of macrophages with AHL was able to
only partly elevate phagocytosis of bacteria, suggesting that other
factors directly or indirectly controlled by *lasI/rhlI* may play
a larger role in this event (**Figure 2**). Also, this partial effect
can be explained by donor-specific variations in macrophage
population that display different capacities and functions,
including migration and phagocytosis.

Indeed, 3O-C_{12}-HSL signal molecules did modulate the level
of phagocytosis of yeast particles by macrophages but this was
not accompanied by an enhanced respiratory or oxidative burst
(Vikström et al., 2005). It is of course also a risk for the host, if the
bacteria survive intracellularly. Neutrophils, always appearing
at an early stage of infection, can sense 3O-C_{12}-HSL and 3O-
C_{10}-HSL and are strongly stimulated to perform chemotaxis,
directional migration (Karlsson et al., 2012) and phagocytosis
(Wagner et al., 2007). Interestingly, AHL affect the migration
and phagocytosis in a time- and dose- dependent manner.
The discrepancies we observe between the different MOI could
perhaps in part be explained by the different concentrations of
AHL. Later in the presence of mature *P. aeruginosa* biofilms,
phagocytes may fail in their orientation and ROS production and
migrate on the extracellular polymeric surface of biofilms in a
disoriented manner (Bylund et al., 2006; Hansch et al., 2008).
The bacteria, on the other hand, might continue to respond
aggressively to the presence of leukocytes by up-regulating the
production of a number of QS-controlled virulence factors,
including rhamnolipids (Jensen et al., 2007), pyocyanine (Allen
et al., 2005), and exopolysaccharides (Bylund et al., 2006),
which then surround the biofilm and affect incoming immune
cells. Moreover, 3O-C_{12}-HSL signals have been shown to down-
regulate the production of the proinflammatory cytokine TNF-
alfa (Telford et al., 1998) and anti-inflammatory cytokine
IL-10 in macrophages (Glucksam-Galnoy et al., 2013) and
increase IL-8 synthesis in bronchial epithelial cells, leading to
massive infiltration of leukocytes (Smith et al., 2001). These
bacterial traits illustrate the complex array of QS-dependent
communication through which opportunistic bacteria can resist
clearance, immune defense, and establish a chronic infection and
destructive inflammation.

A first direct evidence for the involvement of AQP in
physiological cell migration was made by Loitto et al. (2002), who
detected lamellipodial localization of AQP9 during migration.
The concentration of a fluorescent cytoplasmic marker was
diluted in developing protrusions, indicating a localized influx

FIGURE 8 | Proposed model. *P. aeruginosa lasI/rhlI* quorum sensing genes promote phagocytosis and AQP9 redistribution to the leading and trailing regions in macrophages. The phagocytosis of *P. aeruginosa* by macrophages seems more effective when QS genes *lasI* and *rhlI* responsible for synthesis of two QS molecules 3O-C_{12}-HSL and C_4-HSL and associated virulence factors are fully functional. Moreover, the *P. aeruginosa* infections results in elevated AQP9 expression and relocalization to the leading and trailing regions in macrophages, increased cell area, and length; here, bacteria with a functional QS system *lasI/rhlI* achieved stronger responses.

of water. It was proposed that AQP9 can promote membrane extension by a parallel influxes of water and ions that would then create an increased hydrostatic pressure, forcing the membrane to expand and allowing rapid actin polymerization to fill in a protrusion (Loitto et al., 2002, 2009; Saadoun et al., 2005). Accordingly, we decided to investigate the role of AQP9 during bacterial infection. Indeed, using different imaging technology, we observe that *P. aeruginosa* infection results in increased cellular distribution and re-localization of AQP9 to the leading and trailing regions in human macrophages (**Figures 4**, **6**) and in parallel, distinct changes in macrophage cell size and morphology (**Figure 5**), that could facilitate motility, migration, and phagocytosis. Remarkably, the bacteria with functional QS system seemed to contribute more to these processes, illustrating the complex array events in host-pathogen communication, potentially contributing to different outcomes of infections and inflammations (**Figure 8**).

Furthermore, treatment with wild type *P. aeruginosa* and *lasI-/rhlI-* mutant caused significant increase in expression of AQP9 on protein level compared to non-infected control macrophages (**Figure 3**), supporting our imaging results. On the contrary, mRNA level for AQP9 maintains at the basal expression level (**Table S1**). The same pattern was detected for AQP4, 5, 6, 7, and 10 while mRNA levels for AQP0, 1, 2, 3, 8, 11, and 12 were slightly affected. It is worth noting, that a strict correlation between gene and protein expressions may not be seen due to the

control at many levels, including transcriptional and translational regulation (Vogel and Marcotte, 2012). Among such regulator, small non-coding RNA, or microRNA are induced upon *P. aeruginosa* infection, facilitate survival of bacteria in lung cells (Zhou et al., 2014), target AQP5 and induce lung tissue damage (Zhang et al., 2014).

The classical role of AQP to mediate trans-epithelial fluid transport is well-understood, for example in the urinary concentration mechanisms and gland fluid secretion. AQP are also involved in a variety of other physiological and cellular processes, such as swelling of tissues, neural signal transduction, fat metabolism, cell volume regulation, cell migration, and organelle physiology (Verkman, 2005). A few studies have raised the possibility that AQP are important for immune and epithelial cell function during infection. Thus, deletion of AQP5 in alveolar epithelia led to increased bacterial blood dissemination, reduced mucin production in the lung and aggravated lung injury during *P. aeruginosa* infection, speaking for a protective role of AQP5 (Zhang et al., 2011). Furthermore, during pulmonary adenoviral infection, the levels of AQP1 and 5 were decreased and associated with worsened fluid fluxes (Towne et al., 2000). AQP2 and 3 were proposed to contribute to diarrhea caused by Gram-negative bacteria (Guttman et al., 2007). AQP9 was involved in LPS-induced blood-brain barrier permeability and brain water content (Wang et al., 2009), and identified as a potential marker of chronic inflammation in patients with several

different autoimmune diseases (Mesko et al., 2010). In this report, we have discovered and added one more player to infection and inflammatory events, since we noted that *P. aeruginosa* specially one with a working QS system *lasI/rhlI* induces increased AQP9 expression, re-organization and changes in macrophage size.

To conclude, our study demonstrates that the phagocytosis of *P. aeruginosa* by macrophages is more effective when the QS genes *lasI* and *rhlI* being responsible for synthesis of 3O-C$_{12}$-HSL and C$_4$-HSL, and associated virulence factors are fully functional. Moreover, the *P. aeruginosa* infections resulted in elevated AQP9 expression and re-localization to the leading and trailing regions in macrophages, increased cell area and length; bacteria with a working QS system *lasI/rhlI* contributed greater to this process (**Figure 8**). These events may have an influence on the outcome of infection, inflammation, and subsequent development of disease.

Author Contributions

AH has planned and carried out experiments, analyzed the data, evaluated results, and prepared the manuscript. TK evaluated results and prepared the paper. EV is PI of the project, has designed the study, planned, and done experiments, evaluated results, wrote, and finalized the manuscript.

Acknowledgments

Supplementary Material

The Supplementary Material for this article can be found online at: http://journal.frontiersin.org/article/10.3389/fmicb.2015.00915

Figure S1 | The number of adherent and ingested wild type *P. aeruginosa* and its *lasI-/rhlI-* mutant by individual human macrophage. Macrophages were infected with GFP-labeled wild type *P. aeruginosa* or *lasI-/rhlI-* mutant, stained and analyzed by confocal microscopy as shown in **Figure 1**. **(A)** Quantification of the number of ingested bacteria per macrophage. **(B)** Quantification of the number of bound and ingested bacteria (macrophage-associated bacteria) per individual macrophage. Shown are the mean ± SE of seven independent experiments performed at separate days from different blood donors (color coded and same donors as in **Figures 1B,C**). The means ± SE are based on 100–200 cells for each condition per experiment

Figure S2 | Super-resolution SIM imaging of AQP9 in macrophages infected with wild type *P. aeruginosa* and its QS mutant. Macrophages were infected with GFP-labeled (green) wild type *P. aeruginosa,* the *lasI-/rhlI-* mutant or non-infected (Control), for 1 h. Cells were fixed and stained with antibodies against *P. aeruginosa* (blue), rabbit anti-AQP9 and Atto 647N goat anti-rabbit (red) and analyzed by SIM. Bacteria shown in green in these images were completely ingested. Bar 5 µm.

Table S1 | Changes in AQP mRNA levels for macrophages treated with wild type *P. aeruginosa* PAO1 or its *lasI-/rhlI-* mutant at MOI 1, 10 and 100 for 1h compared to levels for the control untreated cells.

References

Allen, L., Dockrell, D. H., Pattery, T., Lee, D. G., Cornelis, P., Hellewell, P. G., et al. (2005). Pyocyanin production by *Pseudomonas aeruginosa* induces neutrophil apoptosis and impairs neutrophil-mediated host defenses *in vivo*. *J. Immunol.* 174, 3643–3649. doi: 10.4049/jimmunol.174.6.3643

Benga, G. (2012). On the definition, nomenclature and classification of water channel proteins (aquaporins and relatives). *Mol. Aspects Med.* 33, 514–517. doi: 10.1016/j.mam.2012.04.003

Blom, H., and Brismar, H. (2014). STED microscopy: increased resolution for medical research? *J. Intern. Med.* 276, 560–578. doi: 10.1111/joim.12278

Brint, J. M., and Ohman, D. E. (1995). Synthesis of multiple exoproducts in *Pseudomonas aeruginosa* is under the control of RhlR-RhlI, another set of regulators in strain PAO1 with homology to the autoinducer-responsive LuxR-LuxI family. *J. Bacteriol.* 177, 7155–7163.

Bylund, J., Burgess, L. A., Cescutti, P., Ernst, R. K., and Speert, D. P. (2006). Exopolysaccharides from *Burkholderia cenocepacia* inhibit neutrophil chemotaxis and scavenge reactive oxygen species. *J. Biol. Chem.* 281, 2526–2532. doi: 10.1074/jbc.M510692200

Chhabra, S. R., Harty, C., Hooi, D. S., Daykin, M., Williams, P., Telford, G., et al. (2003). Synthetic analogues of the bacterial signal (quorum sensing) molecule N-(3-oxododecanoyl)-L-homoserine lactone as immune modulators. *J. Med. Chem.* 46, 97–104. doi: 10.1021/jm020909n

Cullen, L., and McClean, S. (2015). Bacterial adaptation during chronic respiratory infections. *Pathogens* 4, 66–89. doi: 10.3390/pathogens4010066

de Kievit, T. R. (2009). Quorum sensing in *Pseudomonas aeruginosa* biofilms. *Environ. Microbiol.* 11, 279–288. doi: 10.1111/j.1462-2920.2008.01792.x

Gambello, M. J., and Iglewski, B. H. (1991). Cloning and characterization of the *Pseudomonas aeruginosa* lasR gene, a transcriptional activator of elastase expression. *J. Bacteriol.* 173, 3000–3009.

Gambello, M. J., Kaye, S., and Iglewski, B. H. (1993). LasR of *Pseudomonas aeruginosa* is a transcriptional activator of the alkaline protease gene (apr) and an enhancer of exotoxin A expression. *Infect. Immun.* 61, 1180–1184.

Glucksam-Galnoy, Y., Sananes, R., Silberstein, N., Krief, P., Kravchenko, V. V., Meijler, M. M., et al. (2013). The bacterial quorum-sensing signal molecule N-3-oxo-dodecanoyl-L-homoserine lactone reciprocally modulates pro- and anti-inflammatory cytokines in activated macrophages. *J. Immunol.* 191, 337–344. doi: 10.4049/jimmunol.1300368

Guttman, J. A., Samji, F. N., Li, Y., Deng, W., Lin, A., and Finlay, B. B. (2007). Aquaporins contribute to diarrhoea caused by attaching and effacing bacterial pathogens. *Cell Microbiol.* 9, 131–141. doi: 10.1111/j.1462-5822.2006.00773.x

Hansch, G. M., Brenner-Weiss, G., Prior, B., Wagner, C., and Obst, U. (2008). The extracellular polymer substance of *Pseudomonas aeruginosa*: too slippery for neutrophils to migrate on? *Int. J. Artif. Organs.* 31, 796–803. Available online at: http://www.artificial-organs.com

Holm, A., and Vikström, E. (2014). Quorum sensing communication between bacteria and human cells: signals, targets, and functions. *Front. Plant Sci.* 5:309. doi: 10.3389/fpls.2014.00309

Ishibashi, K., Hara, S., and Kondo, S. (2009). Aquaporin water channels in mammals. *Clin. Exp. Nephrol.* 13, 107–117. doi: 10.1007/s10157-008-0118-6

Jarosz, L. M., Ovchinnikova, E. S., Meijler, M. M., and Krom, B. P. (2011). Microbial spy games and host response: roles of a *Pseudomonas aeruginosa* small molecule in communication with other species. *PLoS Pathog.* 7:e1002312. doi: 10.1371/journal.ppat.1002312

Jelen, S., Wacker, S., Aponte-Santamaría, C., Skott, M., Rojek, A., Johanson, U., et al. (2011). Aquaporin-9 protein is the primary route of hepatocyte glycerol uptake for glycerol gluconeogenesis in mice. *J. Biol. Chem.* 286, 44319–44325. doi: 10.1074/jbc.M111.297002

Jensen, P. Ø., Bjarnsholt, T., Phipps, R., Rasmussen, T. B., Calum, H., Christoffersen, L., et al. (2007). Rapid necrotic killing of polymorphonuclear leukocytes is caused by quorum-sensing-controlled production of rhamnolipid by *Pseudomonas aeruginosa*. *Microbiology* 153, 1329–1338. doi: 10.1099/mic.0.2006/003863-0

Karlsson, T., Bolshakova, A., Magalhães, M. A., Loitto, V. M., and Magnusson, K. E. (2013a). Fluxes of water through aquaporin 9 weaken membrane-cytoskeleton anchorage and promote formation of membrane protrusions. *PLoS ONE* 8:e59901. doi: 10.1371/journal.pone.0059901

Karlsson, T., Glogauer, M., Ellen, R. P., Loitto, V. M., Magnusson, K. E., and Magalhães, M. A. (2011). Aquaporin 9 phosphorylation mediates membrane localization and neutrophil polarization. *J. Leukoc. Biol.* 90, 963–973. doi: 10.1189/jlb.0910540

Karlsson, T., Lagerholm, B. C., Vikström, E., Loitto, V. M., and Magnusson, K. E. (2013b). Water fluxes through aquaporin-9 prime epithelial cells for rapid wound healing. *Biochem. Biophys. Res. Commun.* 430, 993–998. doi: 10.1016/j.bbrc.2012.11.125

Karlsson, T., Musse, F., Magnusson, K. E., and Vikström, E. (2012). N-Acylhomoserine lactones are potent neutrophil chemoattractants that act via calcium mobilization and actin remodeling. *J. Leukoc. Biol.* 91, 15–26. doi: 10.1189/jlb.0111034

Loitto, V. M., Forslund, T., Sundqvist, T., Magnusson, K. E., and Gustafsson, M. (2002). Neutrophil leukocyte motility requires directed water influx. *J. Leukoc. Biol.* 71, 212–222. Available online at: http://www.jleukbio.org/content/71/2/212.long

Loitto, V. M., Karlsson, T., and Magnusson, K. E. (2009). Water flux in cell motility: expanding the mechanisms of membrane protrusion. *Cell Motil. Cytoskeleton* 66, 237–247. doi: 10.1002/cm.20357

Mesko, B., Poliska, S., Szegedi, A., Szekanecz, Z., Palatka, K., Papp, M., et al. (2010). Peripheral blood gene expression patterns discriminate among chronic inflammatory diseases and healthy controls and identify novel targets. *BMC Med. Genomics* 3:15. doi: 10.1186/1755-8794-3-15

Moré, M. I., Finger, L. D., Stryker, J. L., Fuqua, C., Eberhard, A., Winans, S. C. et al. (1996). Enzymatic synthesis of a quorum-sensing autoinducer through use of defined substrates. *Science* 272, 1655–1658. doi: 10.1126/science.272.5268.1655

Nourshargh, S., and Alon, R. (2014). Leukocyte migration into inflamed tissues. *Immunity* 41, 694–707. doi: 10.1016/j.immuni.2014.10.008

Ochsner, U. A., Koch, A. K., Fiechter, A., and Reiser, J. (1994). Isolation and characterization of a regulatory gene affecting rhamnolipid biosurfactant synthesis in *Pseudomonas aeruginosa*. *J. Bacteriol.* 176, 2044–2054.

Parsek, M. R., Val, D. L., Hanzelka, B. L., Cronan, J. E. Jr., and Greenberg, E. P. (1999). Acyl homoserine-lactone quorum-sensing signal generation. *Proc. Natl. Acad. Sci. U.S.A.* 96, 4360–4365. doi: 10.1073/pnas.96.8.4360

Pearson, J. P., Feldman, M., Iglewski, B. H., and Prince, A. (2000). *Pseudomonas aeruginosa* cell-to-cell signaling is required for virulence in a model of acute pulmonary infection. *Infect. Immun.* 68, 4331–4334. doi: 10.1128/IAI.68.7.4331-4334.2000

Pearson, J. P., Passador, L., Iglewski, B. H., and Greenberg, E. P. (1995). A second N-acylhomoserine lactone signal produced by *Pseudomonas aeruginosa*. *Proc. Natl. Acad. Sci. U.S.A.* 92, 1490–1494. doi: 10.1073/pnas.92.5.1490

Pearson, J. P., Pesci, E. C., and Iglewski, B. H. (1997). Roles of *Pseudomonas aeruginosa* las and rhl quorum-sensing systems in control of elastase and rhamnolipid biosynthesis genes. *J. Bacteriol.* 179, 5756–5767.

Rumbaugh, K. P., Griswold, J. A., Iglewski, B. H., and Hamood, A. N. (1999). Contribution of quorum sensing to the virulence of *Pseudomonas aeruginosa* in burn wound infections. *Infect. Immun.* 67, 5854–5862.

Rutherford, S. T., and Bassler, B. L. (2012). Bacterial quorum sensing: its role in virulence and possibilities for its control. *Cold Spring Harb. Perspect. Med.* 2:a012427. doi: 10.1101/cshperspect.a012427

Saadoun, S., Papadopoulos, M. C., Hara-Chikuma, M., and Verkman, A. S. (2005). Impairment of angiogenesis and cell migration by targeted aquaporin-1 gene disruption. *Nature* 434, 786–792. doi: 10.1038/nature03460

Savage, D. F., and Stroud, R. M. (2007). Structural basis of aquaporin inhibition by mercury. *J. Mol. Biol.* 368, 607–617. doi: 10.1016/j.jmb.2007.02.070

Schuster, M., Lostroh, C. P., Ogi, T., and Greenberg, E. P. (2003). Identification, timing, and signal specificity of *Pseudomonas aeruginosa* quorum-controlled genes: a transcriptome analysis. *J. Bacteriol.* 185, 2066–2079. doi: 10.1128/JB.185.7.2066-2079.2003

Singh, P. K., Schaefer, A. L., Parsek, M. R., Moninger, T. O., Welsh, M. J., and Greenberg, E. P. (2000). Quorum-sensing signals indicate that cystic fibrosis lungs are infected with bacterial biofilms. *Nature* 407, 762–764. doi: 10.1038/35037627

Smith, R. S., Fedyk, E. R., Springer, T. A., Mukaida, N., Iglewski, B. H., and Phipps, R. P. (2001). IL-8 production in human lung fibroblasts and epithelial cells activated by the Pseudomonas autoinducer N-3-oxododecanoyl homoserine lactone is transcriptionally regulated by NF-kappa B and activator protein-2. *J. Immunol.* 167, 366–374. doi: 10.4049/jimmunol.167.1.366

Surette, M. G., and Bassler, B. L. (1998). Quorum sensing in *Escherichia coli* and *Salmonella typhimurium*. *Proc. Natl. Acad. Sci. U.S.A.* 95, 7046–7050. doi: 10.1073/pnas.95.12.7046

Tang, H. B., DiMango, E., Bryan, R., Gambello, M., Iglewski, B. H., Goldberg, J. B., et al. (1996). Contribution of specific *Pseudomonas aeruginosa* virulence factors to pathogenesis of pneumonia in a neonatal mouse model of infection. *Infect. Immun.* 64, 37–43.

Telford, G., Wheeler, D., Williams, P., Tomkins, P. T., Appleby, P., Sewell, H., et al. (1998). The *Pseudomonas aeruginosa* quorum-sensing signal molecule N-(3-oxododecanoyl)-L-homoserine lactone has immunomodulatory activity. *Infect. Immun.* 66, 36–42.

Teplitski, M., Mathesius, U., and Rumbaugh, K. P. (2011). Perception and degradation of N-acyl homoserine lactone quorum sensing signals by mammalian and plant cells. *Chem. Rev.* 111, 100–116. doi: 10.1021/cr100045m

Toder, D. S., Gambello, M. J., and Iglewski, B. H. (1991). *Pseudomonas aeruginosa* LasA: a second elastase under the transcriptional control of lasR. *Mol. Microbiol.* 5, 2003–2010. doi: 10.1111/j.1365-2958.1991.tb00822.x

Towne, J. E., Harrod, K. S., Krane, C. M., and Menon, A. G. (2000). Decreased expression of aquaporin (AQP)1 and AQP5 in mouse lung after acute viral infection. *Am. J. Respir. Cell Mol. Biol.* 22, 34–44. doi: 10.1165/ajrcmb.22.1.3818

Verkman, A. S. (2005). More than just water channels: unexpected cellular roles of aquaporins. *J. Cell Sci.* 118, 3225–3232. doi: 10.1242/jcs.02519

Vikström, E., Magnusson, K. E., and Pivoriunas, A. (2005). The *Pseudomonas aeruginosa* quorum-sensing molecule N-(3-oxododecanoyl)-L-homoserine lactone stimulates phagocytic activity in human macrophages through the p38 MAPK pathway. *Microbes Infect.* 7, 1512–1518. doi: 10.1016/j.micinf.2005.05.012

Vogel, C., and Marcotte, E. M. (2012). Insights into the regulation of protein abundance from proteomic and transcriptomic analyses. *Nat. Rev. Genet.* 13, 227–232. doi: 10.1038/nrg3185

Wacker, S. J., Aponte-Santamaría, C., Kjellbom, P., Nielsen, S., de Groot, B. L., Rützler, M. et al. (2013). The identification of novel, high affinity AQP9 inhibitors in an intracellular binding site. *Mol. Membr. Biol.* 30, 246–260. doi: 10.3109/09687688.2013.773095

Wagner, C., Zimmermann, S., Brenner-Weiss, G., Hug, F., Prior, B., Obst, U., et al. (2007). The quorum-sensing molecule N-3-oxododecanoyl homoserine lactone (3OC12-HSL) enhances the host defence by activating human polymorphonuclear neutrophils (PMN). *Anal. Bioanal. Chem.* 387, 481–487. doi: 10.1007/s00216-006-0698-5

Wang, H., Jin, R., Tian, P., and Zhuo, Z. (2009). Enhanced expression of aquaporin-9 in rat brain edema induced by bacterial lipopolysaccharides. *J. Huazhong Univ. Sci. Technolog. Med. Sci.* 29, 150–155. doi: 10.1007/s11596-009-0203-4

Williams, P., and Cámara, M. (2009). Quorum sensing and environmental adaptation in *Pseudomonas aeruginosa*: a tale of regulatory networks and multifunctional signal molecules. *Curr. Opin. Microbiol.* 12, 182–191. doi: 10.1016/j.mib.2009.01.005

Zhang, Y., Chen, M., Zhang, Y., Peng, P., Li, J., and Xin, X. (2014). miR-96 and miR-330 overexpressed and targeted AQP5 in lipopolysaccharide-induced rat lung damage of disseminated intravascular coagulation. *Blood Coagul. Fibrinolysis* 25, 731–737. doi: 10.1097/MBC.0000000000000133

Zhang, Z. Q., Song, Y. L., Chen, Z. H., Shen, Y., and Bai, C. X. (2011). Deletion of aquaporin 5 aggravates acute lung injury induced by *Pseudomonas*

aeruginosa. J. Trauma. 71, 1305–1311. doi: 10.1097/TA.0b013e31821 28528

Zhou, X., Li, X., Ye, Y., Zhao, K., Zhuang, Y., Li, Y., et al. (2014). MicroRNA-302b augments host defense to bacteria by regulating inflammatory responses via feedback to TLR/IRAK4 circuits. *Nat. Commun.* 5, 3619. doi: 10.1038/ncomms4619

Zimmermann, S., Wagner, C., Müller, W., Brenner-Weiss, G., Hug, F., Prior, B., et al. (2006). Induction of neutrophil chemotaxis by the quorum-sensing molecule N-(3-oxododecanoyl)-L-homoserine lactone. *Infect. Immun.* 74, 5687–5692. doi: 10.1128/IAI.01940-05